

# Large converse magnetoelectric coupling in FeCoV/lead zinc niobate-lead titanate heterostructure

Yajie Chen,<sup>1,a)</sup> Jinsheng Gao,<sup>1</sup> Trifon Fitchorov,<sup>1</sup> Zhuhua Cai,<sup>2</sup> K. S. Ziemer,<sup>2</sup> Carmine Vittoria,<sup>1</sup> and V. G. Harris<sup>1</sup>

<sup>1</sup>Department of Electrical and Computer Engineering and Center for Microwave Magnetic Materials and Integrated Circuits, Northeastern University, Boston, Massachusetts 02115, USA

<sup>2</sup>Department of Chemical Engineering, Northeastern University, Boston, Massachusetts 02115, USA

(Received 2 January 2009; accepted 3 February 2009; published online 25 February 2009)

Multiferroic behavior was directly verified in a laminated ferroelectric-ferromagnetic heterostructure consisting of a FeCoV thick film (70  $\mu\text{m}$ ) and lead zinc niobate-lead titanate (PZN-PT) single crystal. This unique heterostructure demonstrates a significant converse magnetoelectric (CME) effect corresponding to a CME coupling constant of 31 Oe/kV  $\text{cm}^{-1}$ . It derives from the soft magnetic and magnetostrictive properties ( $\lambda=60$  ppm) of FeCoV alloy and the superior electromechanical properties ( $d_{32}=-2800$  pC/N) of PZN-PT crystal. The electric field controlled magnetic hysteresis is discussed in terms of a stress-induced anisotropy field model. The theoretical calculation is within 7% of the measured induced field of 240 Oe. © 2009 American Institute of Physics. [DOI: 10.1063/1.3086879]

Interest in the magnetoelectric (ME) effect can be dated back to the 1950s.<sup>1</sup> However, during the past decade, multiferroic ME materials have attracted renewed interest for both their fundamental physical properties and in potential applications as memories, sensors, transducers, etc.<sup>2,3</sup> Multiferroic materials are classified as either single phase or multiphase multiferroics. However, because spin and/or charge ordering temperatures remain far below room temperature, and only in response to high applied magnetic or electric fields, single phase multiferroic compounds,<sup>4</sup> remain more a scientific curiosity than as viable engineering materials.

In comparison to single phase multiferroics, the multi-component structured composites, generally consisting of a ferromagnetic phase and a ferroelectric phase, are able to demonstrate considerably stronger ME couplings at room temperature and therefore have become of intense interest to the ferroelectrics and magnetics communities.<sup>5,6</sup>

These artificial heterostructures or multicomponent granular composites bring unique opportunities in realizing many practical applications, such as voltage-controlled magnetic memory elements, ferromagnetic resonance devices, low-frequency room temperature sensor arrays, and transducers with magnetically modulated piezoelectricity.<sup>7,8</sup> In recent years, in particular, there has been a large body of research on multiferroic heterostructures<sup>9–11</sup> that employ a wide range of magnetostrictive and ferroelectric materials, including the first ME heterostructures based on semiconductor substrates (e.g., GaAs).<sup>12</sup>

In this letter, we report a new multiferroic heterostructure consisting of the FeCoV alloy thick film and lead zinc niobate-PT (PZN-PT) single crystal. In contrast to prototypical ME constructs, this system demonstrates significant converse ME (CME) coupling, which is defined as a change in magnetization due to an external electric field. This effect was verified by static magnetic measurements using a vibrating sample magnetometry (VSM) under the application of electric fields as opposed to the more common measurement

by ac modulation or ferromagnetic resonance.

FeCoV alloys possess superior magnetic and mechanical properties at elevated temperatures and have found use in magnetic bearings, transformers, and electrical generators that operate under high stress and at high temperatures.<sup>13</sup> In the present study, a 350  $\mu\text{m}$  thick  $\text{Fe}_{48}\text{Co}_{50}\text{V}_2$  cold-rolled strip was employed as the magnetostrictive element. To gain an optimum combination of mechanical and magnetic properties, the FeCoV alloy was heat treated at 600 to 700 °C in a  $\text{H}_2$  gas atmosphere and polished to a 70  $\mu\text{m}$  thickness.

To produce strong ME coupling in the proposed heterostructure, it was crucial to select a high functioning piezoelectric crystal as the substrate. We chose a relaxor-based ferroelectric single crystal,  $\text{Pb}(\text{Zn}_{1/3}\text{Nb}_{2/3})\text{O}_3\text{-PbTiO}_3$ , consisting of a rhombohedral symmetric PZN and a tetragonal symmetry ferroelectric PT. This crystal features exceptional dielectric and electromechanical properties: e.g.,  $k_{33}=0.86$ ,  $d_{31}=1100$  pC/N,  $d_{32}=-2700\text{--}3200$  pC/N,  $d_{33}=1500$  pC/N,  $K^T>5000$ , and  $\tan \delta<0.01$  at 1 kHz.<sup>14</sup>

Finally, this multiferroic heterostructure was designed to operate in the L-T ME coupling mode (i.e., longitudinal magnetized/transverse polarized) and consisted of a laminated structure of a FeCoV film and PZN-6%PT single crystal poled along the [011] direction. The two components were bonded with quick curing ethyl cyanoacrylate. The magnetic properties were measured using a Lakeshore vibrating sample magnetometer with the magnetic field direction aligned parallel to the [100] direction ( $d_{32}$ ). Electric fields from  $\sim+8$  to 8 kV/cm were applied across two electrodes. Each electrode consists of NiCr (25–40 nm) and AuPd (250 nm) layers. Measurement for the CME coupling was performed in the field and geometry configurations depicted in Fig. 1(a). An external magnetic field ( $H$ ) was applied along the [100] ( $d_{32}$ ) direction of the PZN-PT crystal, whereas the [011] ( $d_{33}$ ) is perpendicular to the heterostructure plane. The thicknesses of the FeCoV film and PZN-PT crystal were 70 and 500  $\mu\text{m}$ , respectively. The optimized ratio of thickness is a prerequisite in obtaining large CME coupling.<sup>3</sup>

<sup>a)</sup>Electronic mail: y.chen@neu.edu.

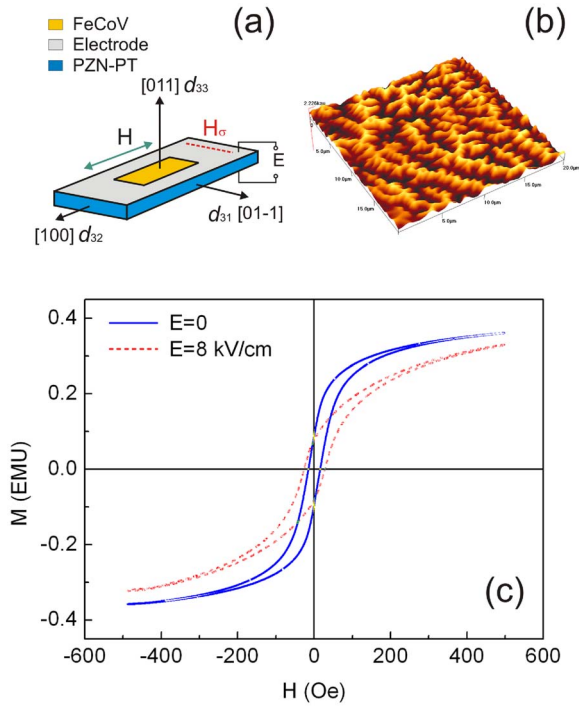


FIG. 1. (Color online) (a) Schematic diagram of the FeCoV/PZN-PT multiferroic heterostructure, (b) 3D magnetic domain image for FeCoV film by MFM, and (c) magnetic hysteresis loops under application of an electric field strength  $E=8$  kV/cm (dash line: ----) and no electric field (solid line: —).

Figure 1(b) depicts a three-dimensional magnetic force microscopy (MFM) image illustrating the morphology of the magnetic domain structure of the FeCoV film. It reveals a branched domain pattern common to Co-based magnetic alloys.<sup>15</sup> Figure 1(c) presents basic static magnetic properties measured by VSM. The magnetic film has a saturation magnetization  $4\pi M_s$  of  $20 \pm 0.2$  kG ( $H=10$  kOe) and a coercivity  $H_c$  of 15 Oe in the absence of an electric bias field. The application of an electric field results in significant changes to magnetic hysteresis. This phenomenon will be discussed below.

The correlation between magnetization ( $M$  at  $H=500$  Oe) and electric field is presented in Fig. 2(a). The typical butterfly-shaped loop is associated with the dependence of strain on electric field in the PZN-PT crystal.<sup>16</sup> This result stems from ferroelectric hysteresis. It is evident that the  $M$ - $E$  curve corresponds closely to the ferroelectric hysteresis loop ( $P$ - $E$  curve), as depicted in Fig. 2 (dashed line). It is noteworthy that the electric coercivity ( $E_c$ ) is about 5.2 kV/cm, which results in two shoulders in the  $M$ - $E$  curve. Clearly, the application of electric field results in a reduction in magnetization by 10%. Figure 2(b) illustrates the variations in remanence ( $M_r$ ) and magnetization loop squareness (SQ) with the application of an electric field. The remanent magnetization and loop SQ display a complicated dependence with applied electric field, which contains two broad peaks in the vicinity of 5–7 kV/cm. In this heterostructure, the induced magnetic field obtained is based on the so-called Villari effect, i.e., a reverse magnetostriction.<sup>17</sup> Due to the hysteresis behavior of ferromagnetic materials, the magnetostriction process also exhibits hysteresis, which strongly mirrors the magnetization process. Furthermore, it is assumed that the appearance of the peaks is associated with both the nonlinear relationships between strain and stress, and strain

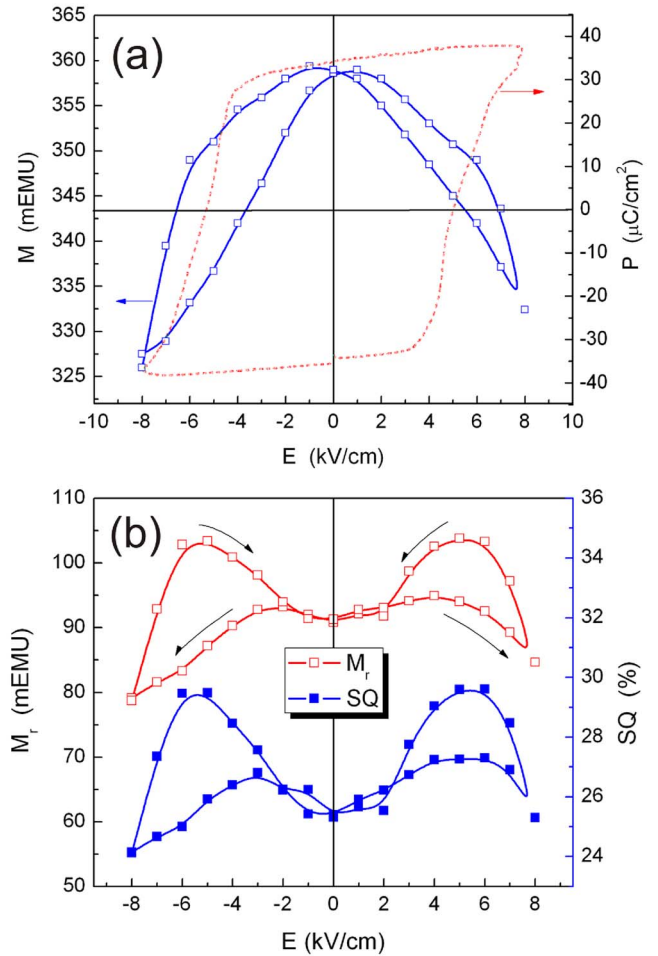


FIG. 2. (Color online) (a) Dependence of magnetization ( $M$ ) at  $H=500$  Oe on the applied electric field ( $E$ ) in the laminated FeCoV/PZN-PT heterostructure (solid line: —) and the polarization hysteresis loop for the ferroelectric PZN-PT crystal used in the heterostructure (dash line: ----). (b) Variation in remanence ( $M_r$ ) and SQ under an electric field strength ( $E$ ) for the FeCoV/PZN-PT heterostructure.

and electric field, in the PZN-PT crystal.<sup>18,19</sup> Previous work indicated a complex relationship between magnetic hysteresis and stress even in the absence of an electric bias field.<sup>20,21</sup> Nevertheless, a maximum electric field tunability in both remanence and SQ of 37% and 23%, respectively, was demonstrated in response to a 2 kV/cm change in electric field strength.

Figure 3(a) presents the electric field dependence of magnetic coercivity ( $H_c$ ) for the FeCoV film. This clearly shows an irreversible loop similar to the  $M$ - $E$  loop depicted in Fig. 2. Coercivity  $H_c$  dramatically increases from 15.2 to 26.5 Oe with an applied electric field of 8 kV/cm. This corresponds to an increase of 71% and a coercivity tunability of  $1.4$  Oe/kV  $\text{cm}^{-1}$  or  $9\%$ /kV  $\text{cm}^{-1}$ . The correlation between coercivity and electric field was not adequately addressed in previous ME studies; however, it essentially reflects the dependence of coercivity upon stress, which has been extensively studied.<sup>22,23</sup> As a result, a stress dependence of coercivity is determined by the following factors: (1) the direction of the stress-induced field ( $H_p^E$ ) relative to an external field ( $H$ ), (2) the coercivity mechanism, i.e., irreversible rotation or domain wall displacement, and (3) the stress-induced change in the orientation, magnitude, and distribution of magnetic anisotropy fields. Here,  $H_p^E$  is assumed to be

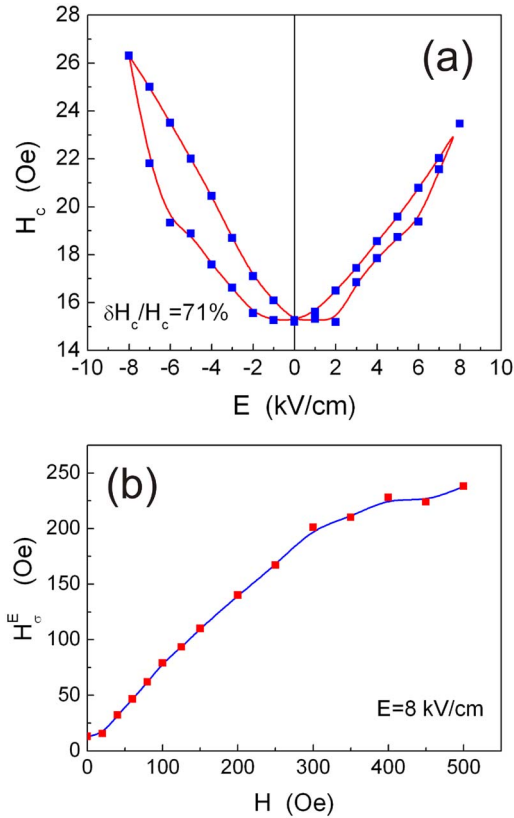


FIG. 3. (Color online) (a) Dependence of coercivity ( $H_c$ ) on an electric field strength ( $E$ ) and (b) correlation between the stress-induced magnetic field ( $H_c^E$ ) and external magnetic field ( $H$ ) for the FeCoV/PZN-PT heterostructure.

perpendicular to  $H$ , and the coercivity is predominately attributed to irreversible domain wall motion, which is evident in the field configurations and magnetic domain patterns of Figs. 1(a) and 1(b). These results clearly illustrate an increase in coercivity in response to an electric bias field, where a compressive stress results in a large enhancement in coercivity that was not predicted or measured in earlier studies.<sup>22</sup>

It is understandable that the stress-induced anisotropy field is critical in determining the coercivity of the magnetic material. We therefore attempt to calculate the stress-induced field in the FeCoV film by considering the strain inside the PZN-PT crystal created by application of the electric bias field. This induced field is expressed as<sup>24</sup>

$$H_{\sigma}^E = \frac{3}{\partial M} \frac{\partial \lambda}{\partial M} \sigma (\cos^2 \varphi - \nu \sin^2 \varphi), \quad (1)$$

where  $\varphi$  is the angle between magnetization and stress and  $\nu$  denotes Poisson ratio of the magnetic material. In this structure,  $\varphi$  and  $\nu$  are  $90^\circ$  and 0.41, respectively. The magnetostriction coefficient ( $\lambda$ ) and saturation magnetization ( $M_s$ ) are 60 ppm and 1590 G, respectively. The stress ( $\sigma$ ) in the FeCoV film is roughly derived from a simple relation:  $\sigma = d_{32} E Y$ , where  $Y$  (the Young's modulus) is  $2 \times 10^{12}$  dyn/cm<sup>2</sup>,<sup>25</sup>  $d_{32} = -2800$  pC/N, and  $E = 8$  kV/cm. Applying these relations, the stress-induced field is

$H_{\sigma}^E = -224$  Oe, where a negative sign represents the induced field transverse to an external field (the magnetization direction)<sup>22</sup> [see Fig. 1(b)]. In fact, a larger estimate of the induced field  $H_{\sigma}^E$  can be expected because  $H_{\sigma}^E$  depends on  $\partial \lambda / \partial M$ .

Figure 3(b) shows the correlation between external magnetic field and stress-induced magnetic field, which was extracted from Fig. 1(c). A significant increase in the induced field emerges in the external fields below 300 Oe. It is potentially valuable that an 8 kV/cm electric field strength enables the heterostructure to generate an induced magnetic field of  $\sim 240$  Oe under a small biased magnetic field. This corresponds to a CME coupling constant of  $31$  Oe/kV cm<sup>-1</sup>, which is among the largest values reported for ME heterostructures.<sup>7</sup> It is also noticed that the measured value is very close to the estimated value of 224 Oe. Additionally, the CME coupling is likely to be enhanced by employing an epoxy having a Young's modulus close to the magnetic material instead of the ethyl cyanoacrylate employed here.

This work was supported by the Office of Naval Research under Grant No. N00014-05-1-0349.

<sup>1</sup>W. Prellier, M. P. Singh, and P. Murugavel, *J. Phys.: Condens. Matter* **17**, R803 (2005).

<sup>2</sup>R. Ramesh and N. A. Spaldin, *Nature Mater.* **6**, 21 (2007).

<sup>3</sup>C. W. Nan, M. I. Bichurin, S. Dong, and D. Viehland, *J. Appl. Phys.* **103**, 031101 (2008).

<sup>4</sup>T. Kimura, *Annu. Rev. Mater. Res.* **37**, 387 (2007).

<sup>5</sup>W. Eerenstein, M. Wiora, J. L. Prieto, J. F. Scott, and N. D. Mathur, *Nature Mater.* **6**, 348 (2007).

<sup>6</sup>M. Liu, X. Li, H. Imrane, Y. Chen, T. Goodrich, K. S. Ziemer, J. Y. Huang, and N. X. Sun, *Appl. Phys. Lett.* **90**, 152501 (2007).

<sup>7</sup>J. Scott, *Nature Mater.* **6**, 256 (2007).

<sup>8</sup>M. I. Bichurin, I. A. Kornev, V. M. Petrov, A. S. Tatarenko, Yu. V. Kiliba, and G. Srinivasan, *Phys. Rev. B* **64**, 094409 (2001).

<sup>9</sup>Y. Chen, J. Wang, M. Liu, J. Lou, N. X. Sun, C. Vittoria, and V. G. Harris, *Appl. Phys. Lett.* **93**, 112502 (2008).

<sup>10</sup>D. A. Filippov, G. Srinivasan, and A. Gupta, *J. Phys.: Condens. Matter* **20**, 425206 (2008).

<sup>11</sup>S. Dong, J. F. Li, and D. Viehland, *Appl. Phys. Lett.* **83**, 2265 (2003).

<sup>12</sup>Y. Chen, J. Gao, J. Lou, M. Liu, S. D. Yoon, A. L. Geiler, M. Nedoroscik, D. Heiman, N. X. Sun, C. Vittoria, and V. G. Harris, *J. Appl. Phys.* **105**, 07A510 (2009).

<sup>13</sup>C. H. Shang, T. P. Weihs, R. C. Cammarata, Y. Ji, and C. L. Chien, *J. Appl. Phys.* **87**, 6508 (2000).

<sup>14</sup>K. K. Rajan, M. Shanthy, W. S. Chang, J. Jin, and L. C. Lim, *Sens. Actuators, A* **133**, 110 (2007).

<sup>15</sup>A. Hubert and R. Schäfer, *Magnetic Domain: The Analysis of Magnetic Microstructures* (Springer, Berlin, 1998).

<sup>16</sup>L. C. Lim, K. K. Rajan, and J. Jin, *IEEE Trans. Ultrason. Ferroelectr. Freq. Control* **54**, 2474 (2007).

<sup>17</sup>G. Engdahl, *Handbook of Giant Magnetostrictive Materials* (Academic, San Diego, 2000).

<sup>18</sup>X. Ren, *Nature Mater.* **3**, 91 (2004).

<sup>19</sup>A. Amin, E. McLaughlin, H. Robinson, and L. Ewart, *IEEE Trans. Ultrason. Ferroelectr. Freq. Control* **54**, 1090 (2007).

<sup>20</sup>H. Hauser, *J. Appl. Phys.* **96**, 2753 (2004).

<sup>21</sup>M. J. Sablik, H. Kwun, G. L. Burkhardt, and D. C. Jiles, *J. Appl. Phys.* **61**, 3799 (1987).

<sup>22</sup>L. Callegaro and E. Puppini, *Appl. Phys. Lett.* **68**, 1279 (1996).

<sup>23</sup>I. J. Garshelis, *J. Appl. Phys.* **73**, 5629 (1993).

<sup>24</sup>M. J. Sablik, S. W. Rubin, L. A. Riley, D. C. Jiles, D. A. Kaminski, and S. B. Biner, *J. Appl. Phys.* **74**, 480 (1993).

<sup>25</sup>Vacuumschmelze catalog, <http://www.vacuumschmelze.de>.